IOPscience iopscience.iop.org

Home Search Collections Journals About Contact us My IOPscience

A new approach to the scattering problem in 2D square-corner discontinuities with an application to the through right-angle bend transmission

This article has been downloaded from IOPscience. Please scroll down to see the full text article.

1993 J. Phys.: Condens. Matter 5 5215

(http://iopscience.iop.org/0953-8984/5/29/017)

View the table of contents for this issue, or go to the journal homepage for more

Download details:
IP Address: 171.66.16.159
The article was downloaded on 12/05/2010 at 14:13

Please note that terms and conditions apply.

J. Phys.: Condens. Matter 5 (1993) 5215–5224. Printed in the UK

A new approach to the scattering problem in 2D square-corner discontinuities with an application to the through right-angle bend transmission

Yuri A Klimenko†, Lyuba I Malysheva‡ and Alexander I Onipko‡

† Glushkov Institute of Cybernetics of the Academy of Science of the Ukraine, Kiev-207, 252207, Ukraine

‡ Bogolyubov Institute for Theoretical Physics of the Academy of Science of the Ukraine, Kiev-143, 252143, Ukraine

Abstract. An exact solution of the scattering problem in 2D square-corner discontinuities is presented in an explicit form. This suggests an efficient computational procedure for characteristics of electron ballistic transport in square-corner shaped waveguides. Using the proposed method, bound-state energies, mode-to-mode as well as total and averaged transmission probabilities, in a square-corner right-angle bend have been calculated. Conductance and electron-filtering properties of the system are found to be challenging problems for its practical realization.

1. Introduction

Partly because of the possibility of device applications, and partly due to some novel phenomena such as existence of bound states in classically unbound systems and modulation of current by quantum interference, wavelike electron transport in two-dimensional (2D) nanostructures has received considerable attention in recent years [1–10]. A number of promising electron waveguide geometries have been examined by means of the recursive Green function method [4], mode matching [1,7–9] and specially designed techniques [2,5,6,10,11]. The scattering problem in these structures is essentially computational, because the mode mixing in the region of the waveguide discontinuities involves an infinite number of the degrees of freedom of the electron motion.

In [2,4–6], the treatment of the electron-scattering region is completely computational. In [1,7–10], the use of an appropriate analytic form for the electron wavefunction in the scattering region rationalizes essentially numerical calculations. Note that only in [9,10], equations for the scattering matrix (in the case of crossed wires) have been presented in an explicit form. In this paper, the analytical description is advanced to present an explicit expression for the exact solution of the scattering problem. Equations (18)–(21) represent this solution and the main result of the work.

Although the derivation of basic equations is performed here for a particular (and deliberately the simplest) waveguide geometry, the form of the obtained equations for the S matrix is canonical, i.e. it is valid for an arbitrary square-corner geometry of discontinuities, including systems with a large number of terminals (the latter case differs simply in the number of equations of the type (18)). Note, in addition, that ballistic transport characteristics in a square-corner right-angle waveguide have already been addressed in the literature [7,11] but only very briefly.

In section 2 we present an analytic solution for the scattering (reflection and transmission) amplitudes in a right-angle bend. General properties of the reflection

0953-8984/93/295215+10$07.50 © 1993 IOP Publishing Ltd

and transmission probabilities are discussed in section 3. In section 4, we investigate the dependence of the bound-state energy in the L-shaped structure on the wire width. Calculations of the transmission characteristics of the right-angle bend are given in section 5, and the main results are briefly summarized in section 6.

2. Statement of the problem and basic equations

Let the electron motion inside a quantum waveguide be governed by the time-independent Schrödinger equation $H\Psi = E\Psi$ with the Hamiltonian (in the tight-binding representation)

$$H = -4L\sum_{R} a_R^+ a_R + L\sum_{R,\delta R} a_R^+ a_{R+\delta R} \tag{1}$$

and the wavefunction

$$\Psi = \sum_{R=(m,n)} \Psi_R a_R^+ |0\rangle. \tag{2}$$

In (1) and (2), a_R^+, a_R are the Fermi creation and annihilation operators of an electron on the site R with coordinates (m, n), δR connects the site R with its nearest neighbours, and L is the overlap integral of electron wavefunctions in the neighbouring sites. Equations for the expansion coefficients Ψ_R can be found by substituting (2) in (1) and multiplying the result by $\langle 0|a_R$, where $|0\rangle$ is the vacuum wavefunction. Note that, by setting the lattice site electron energy in the resulting equations to be equal to $-4L$ with $L = -\hbar^2/2m^*a^2$, (a is the lattice constant, m^* is the effective electronic mass), we make our model, in the continuum limit, completely equivalent to the effective mass approximation [10].

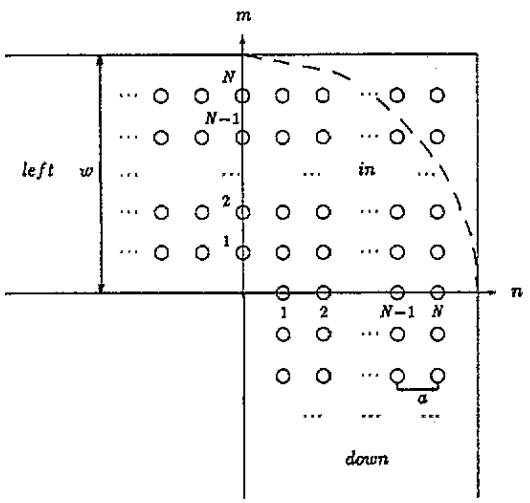

Figure 1. Schematic representation of an L-shaped 2D waveguide. In the lattice, which corresponds to the discrete model of the bend, the lattice-site coordinates m and n (in units of a, the periodicity of the lattice) vary in the interval from $-\infty$ to N. Full lines show the boundary of the waveguide in the continuum limit ($N \to \infty$, Na = constant). In this case, $w = (N + 1)a$ is the waveguide width. The circular right-angle bend with zero inner radius of the bend curvature and with the outer radius equal to w is represented by the dotted curve.

For an L-shaped 2D waveguide, it is convenient to consider the electron wavefunction of the system in each of the three regions, namely, *left*, *in* and *down* (see figure 1), with the following numbering of the lattice sites R: $1 \leqslant m \leqslant N$, $n \leqslant 0$ in the region 'left', $m \leqslant 0$, $1 \leqslant n \leqslant N$ in the region 'down', and $1 \leqslant m \leqslant N$, $1 \leqslant n \leqslant N$ in the region 'in'. In these

regions the expansion coefficients Ψ_R obey the following equations:

$$\frac{E+4L}{L}\Psi_{m,n} = \Psi_{m-1,n}(1-\delta_{m,1}) + \Psi_{m+1,n}(1-\delta_{m,N}) + \Psi_{m,n-1} + \Psi_{m,n+1}$$
$$1 \leqslant m \leqslant N,\ n \leqslant 0 \tag{3}$$

$$\frac{E+4L}{L}\Psi_{m,n} = \Psi_{m-1,n} + \Psi_{m+1,n} + \Psi_{m,n-1}(1-\delta_{n,1}) + \Psi_{m,n+1}(1-\delta_{n,N})$$
$$m \leqslant 0,\ 1 \leqslant n \leqslant N \tag{4}$$

$$\frac{E+4L}{L}\Psi_{m,n} = \Psi_{m-1,n} + \Psi_{m+1,n}(1-\delta_{m,N}) + \Psi_{m,n-1} + \Psi_{m,n+1}(1-\delta_{n,N})$$
$$1 \leqslant m \leqslant N,\ 1 \leqslant n \leqslant N. \tag{5}$$

Stationary solutions to the Schrödinger equation, which describe incident and reflected electron fluxes in the input (left) lead and the transmitted flux in the output (down) lead, can be taken in the form

$$\Psi^{\mathrm{l}}_{m,n} = \sqrt{\frac{2}{N+1}}\sum_{j=1}^{N}\left[\delta_{j,j_0}\exp(\mathrm{i}k_j n) + r_{k_j,k_{j_0}}\exp(-\mathrm{i}k_j n)\right]\sin(\chi_j m) \tag{6}$$

$$\Psi^{\mathrm{d}}_{m,n} = \sqrt{\frac{2}{N+1}}\sum_{j=1}^{N} t_{k_j,kj_0}\exp(-\mathrm{i}k_j m)\sin(\chi_j n) \tag{7}$$

where $\chi_j = \pi j/(N+1)$ is the quantum number of the transverse electron motion, and k_j is the dimensionless longitudinal wavevector of the jth mode. Note that the coefficients (6) and (7) satisfy (3) and (4) except those with $1 \leqslant m \leqslant N$, $n = 0$ and $m = 0$, $1 \leqslant n \leqslant N$, respectively.

The energy of electrons in the waveguide is determined by the mode number j_0 and the wavevector k_{j_0} of the incident flux:

$$E = 2L(\cos\chi_{j_0} + \cos k_{j_0} - 2). \tag{8}$$

While j_0 and k_{j_0} are fixed in the boundary condition of the scattering problem, all other k_j in (6) and (7) are found from the energy conservation law

$$\cos k_{j_0} + \cos\chi_{j_0} = \cos k_j + \cos\chi_j. \tag{9}$$

Solutions to (9) can be either real or imaginary, i.e. the expansions (6) and (7) include propagating and evanescent modes of electronic waves.

In the intersection region of the 'left' and 'down' leads, the electron wavefunction is given by

$$\Psi^{\mathrm{in}}_{m,n} = \sqrt{\frac{2}{N+1}}\sum_{j=1}^{N}[A_{k_j}\exp(\mathrm{i}k_j n) + B_{k_j}\exp(-\mathrm{i}k_j n)]\sin(\chi_j m)$$
$$+\sqrt{\frac{2}{N+1}}\sum_{j=1}^{N}[C_{k_j}\exp(\mathrm{i}k_j m) + D_{k_j}\exp(-\mathrm{i}k_j m)]\sin(\chi_j n). \tag{10}$$

To express the coefficients of the above expansion through the amplitudes of the reflected and transmitted waves, we can use (5) for all the boundary sites of the region in: $1 \leqslant m \leqslant N$, $n = N$; $m = N$, $1 \leqslant n \leqslant N$; $1 \leqslant m \leqslant N$, $n = 1$; $m = 1$, $1 \leqslant n \leqslant N$. This way of

excluding the unknowns A_{k_j}, B_{k_j}, C_{k_j} and D_{k_j} is similar to the matching procedure exploited in the continuous description of the scattering process, but one has to deal with somewhat simpler equations. A more general treatment of square-corner discontinuities offers the Green function technique [10].

Using (10) in (5) for the boundary sites, after some evident algebra we obtain

$$\Psi^{\text{in}}_{m,n} = \sqrt{\frac{2}{N+1}} \sum_{j=1}^{N} (\delta_{j,j_0} + r_{k_j,k_{j_0}}) \frac{\sin[(N+1-n)]k_j}{\sin[(N+1)k_j]} \sin(\chi_j m) + \sqrt{\frac{2}{N+1}} \sum_{j=1}^{N} t_{k_j,k_{j_0}} \frac{\sin[(N+1-m)]k_j}{\sin[(N+1)k_j]} \sin(\chi_j n). \tag{11}$$

The substitution of this expression in (3), (4) for $1 \leqslant m \leqslant N$, $n = 0$ and $m = 0$, $1 \leqslant n \leqslant N$ gives

$$\begin{aligned} Z_j \bar{r}_{k_j,k_{j_0}} &= -2\mathrm{i} \sin k_j \delta_{j,j_0} + \sum_{j'=1}^{N} G_{jj'} t_{k_{j'},k_{j_0}} \\ Z_j t_{k_j,k_{j_0}} &= \sum_{j'=1}^{N} G_{jj'} \bar{r}_{k_{j'},k_{j_0}} \end{aligned} \tag{12}$$

where the following abbreviations are used:

$$\bar{r}_{k_j,k_{j_0}} = \delta_{j,j_0} + r_{k_j,k_{j_0}} \tag{13}$$

$$Z_j = \frac{\sin k_j \exp[-\mathrm{i}(N+1)k_j]}{\sin[(N+1)k_j]} \qquad G_{jj'} = \frac{1}{N+1} \frac{\sin \chi_j \sin \chi_{j'}}{\cos k_j - \cos \chi_{j'}}. \tag{14}$$

Equations (12) are simplified further by introducing the new variables

$$X^{\pm}_{k_j,k_{j_0}} = \bar{r}_{k_j,k_{j_0}} \mp t_{k_j,k_{j_0}} \tag{15}$$

for which

$$Z_j X^{\pm}_{k_j,k_{j_0}} = F_{jj_0} \pm \sum_{j'=1}^{N} G_{jj'} X^{\pm}_{k_{j'},k_{j_0}} \tag{16}$$

or

$$S^{\pm} X^{\pm} = F. \tag{17}$$

In (17), $S^{\pm}_{jj'} = Z_j \delta_{jj'} \mp G_{jj'}$, $X^{\pm} = \mathrm{col}(X^{\pm}_{k_1,k_{j_0}}, \ldots, X^{\pm}_{k_N,k_{j_0}})$, and F is the vector column with the only non-zero element on the j_0th place, $F_{jj_0} = -2\mathrm{i} \sin k_{j_0} \delta_{jj_0}$.

The set (16) can be rewritten in a triangular form

$$\tilde{Z}^{\pm}_j X^{\pm}_{k_j,k_{j_0}} = \tilde{F}^{\pm}_{jj_0} \pm \sum_{j'=1}^{j-1} \tilde{G}^{\pm}_{jj'} X^{\pm}_{k_{j'},k_{j_0}} \tag{18}$$

where the coefficients are defined by the following recurrent relations:

$$\tilde{G}^{\pm}_{jj'} = G_{jj'} \pm \sum_{j''=\max(j,j')+1}^{N} \frac{\tilde{G}^{\pm}_{jj''} \tilde{G}^{\pm}_{j''j'}}{\tilde{Z}^{\pm}_{j''}} \tag{19}$$

$$\tilde{Z}^{\pm}_j = Z_j \mp G_{jj} - \sum_{j'=j+1}^{N} \frac{(\tilde{G}^{\pm}_{jj'})^2}{\tilde{Z}^{\pm}_{j'}} \tag{20}$$

$$\tilde{F}^{\pm}_{jj_0} = -2\mathrm{i} \sin k_{j_0} \delta_{jj_0} + \sum_{j'=j+1}^{N} \frac{\tilde{G}^{\pm}_{jj'} \tilde{F}^{\pm}_{j'j_0}}{\tilde{Z}^{\pm}_{j'}}. \tag{21}$$

Thus, finding solutions to the S-matrix equations is reduced to a simple recurrent procedure. In particular, for low-mode waves, one readily gets

$$X^{\pm}_{k_1,k_{j_0}} = \frac{1}{\tilde{Z}^{\pm}_1}\tilde{F}^{\pm}_{1,j_0}$$

$$X^{\pm}_{k_2,k_{j_0}} = \frac{1}{\tilde{Z}^{\pm}_2}\left(\tilde{F}^{\pm}_{2,j_0} + \frac{\tilde{G}^{\pm}_{21}\tilde{F}^{\pm}_{1j_0}}{\tilde{Z}^{\pm}_1}\right) \tag{22}$$

$$X^{\pm}_{k_3,k_{j_0}} = \frac{1}{\tilde{Z}^{\pm}_3}\left[\tilde{F}^{\pm}_{3,j_0} + \frac{\tilde{G}^{\pm}_{31}\tilde{F}^{\pm}_{1j_0}}{\tilde{Z}^{\pm}_1} + \tilde{G}^{\pm}_{32}\frac{1}{\tilde{Z}^{\pm}_2}\left(\tilde{F}^{\pm}_{2j_0} + \frac{\tilde{G}^{\pm}_{21}\tilde{F}^{\pm}_{1j_0}}{\tilde{Z}^{\pm}_1}\right)\right].$$

The general form of the solution for an arbitrary mode number is evident but unnecessary here.

Since the vector-column $\tilde{F}^{\pm}$ has j_0 non-zero elements, $\tilde{F}^{\pm}_{jj_0} \neq 0$ for $j \leqslant j_0$, expressions for the reflection and transmission amplitudes

$$\begin{Bmatrix} \tilde{r}_{k_j,k_{j_0}} \\ t_{k_j,k_{j_0}} \end{Bmatrix} = \tfrac{1}{2}(X^{+}_{k_j,k_{j_0}} \pm X^{-}_{k_j,k_{j_0}}) \tag{23}$$

become especially simple for the fundamental-mode ($j_0 = 1$) and low-mode propagation.

Thus, (18) suggests, in fact, an explicit form of the exact solution for the discrete model of the L-shaped waveguide. As shown previously [10], the same relations, but with Z_j, $G_{jj'}$ and F_{jj_0} in (18) replaced by $Z^{c}_j = q_j \exp(-i\pi q_j)/\sin(\pi q_j)$, $G^{c}_{jj'} = 2jj'/[\pi(j'^2 - q_j^2)]$, and $F^{c}_{jj_0} = -2iq_j\delta_{jj_0}$, where $q_j = k_j(N+1)/\pi$, can be used, as a solution of the scattering problem for the continuum version of the model, $N \to \infty$, aN = constant. In the latter case ($N = \infty$ in (16)), (18)–(21) represent the desired solution in the N-mode approximation.

The equations obtained above provide an efficient method of calculating the transport properties and bound-state energies of the right-angle bend and similar structures.

3. General properties of scattering probabilities

A characteristic feature inherent in all computational approaches to electron dynamics in quantum waveguides is that the general properties of the system are verified *a posteriori*, using numerical results obtained. Here, some general properties of the reflection and transmission probabilities

$$\begin{Bmatrix} R_{j,j_0} \\ T_{j,j_0} \end{Bmatrix} = \frac{\sin k_j}{\sin k_{j_0}} \begin{Bmatrix} |r_{k_j,k_{j_0}}|^2 \\ |t_{k_j,k_{j_0}}|^2 \end{Bmatrix} \tag{24}$$

which characterize the electron motion in a square-corner right-angle bend, are derived analytically.

The first property, which follows directly from the canonical equations (12), is the flux conservation law

$$\sum_{j=1}^{N_0}(R_{j,j_0} + T_{j,j_0}) = 1 \qquad \text{for all } j_0 \tag{25}$$

where N_0 is the number of modes available for propagation in the channel (i.e. the number of real positive roots of (9) for the given electron energy). It is worth emphasizing that

the equality (25) is strictly held even in the case of the N-mode description of the system, providing that $N > N_0$.

Second, in any dynamic system, forward and backward transitions between system states are not distinguished, and therefore

$$R_{jj_0} = R_{j_0 j} \qquad T_{jj_0} = T_{j_0 j}. \tag{26}$$

The above equality also follows directly from equations (16) for the S matrix.

Third, in the limit $k_{j_0} \to 0$, the set of equations (12) becomes homogeneous, so we have $t_{k_j k_{j_0}} = 0$, $r_{k_j k_{j_0}} = -\delta_{jj_0}$. Thus, all scattering probabilities in this limit are zero except the reflection probability $R_{j_0 j_0} = 1$.

Finally, it can be shown that the equation $t_{k_1,k_1} = 0$, which determines the energy of the resonant reflection in the region of the fundamental-mode propagation, is real. Indeed, since

$$||S^{\pm}|| = (Z_1 \mp G_{11})||S^{\pm}||_{11} + \sum_{j=2}^{N} \pm(-1)^j ||S^{\pm}||_{1j} G_{1j}$$

where $||S^{\pm}||_{jj'}$ is the minor of the matrix $S^{\pm}$ obtained by eliminating the jth row and j'th column, it is easy to see from (17) that the equation $X_{11}^{+} = X_{11}^{-}$ is also real. Therefore, one can expect that the resonant reflection ($T_{11} = 0$) in the fundamental-mode propagation exists. Moreover, the above statement is relevant to any two-terminal structure with square-corner discontinuities and the input and output leads of the same width. This means that the stop-bend behaviour of the device, which obviously has quantum interference origins, is not specific for the right-angle bend but is a general property of two-terminal square-corner structures. Systems with a larger number of terminals, e.g. wire intersections, do not possess this property except the case of a T-shaped waveguide [4]. The latter can act as a two-terminal structure due to its symmetry.

4. Bound states

A remarkable peculiarity of waveguides with square-corner discontinuities is the existence of bound states. The effect, predicted for the first time by Schult and co-workers [1], has a pure quantum nature, since from the classical point of view electrons in waveguides are free and, therefore, cannot be trapped.

In [1], the problem was solved in the framework of the effective mass approximation; here we find the bound-state energies for both the continuum and discrete models. The energies of the bound states correspond to the solutions of the following equation: the determinant of the set (12) equals zero, i.e.

$$\tilde{Z}_1^{+} \tilde{Z}_1^{-} = 0 \tag{27}$$

found outside the continuum spectrum of the system. Thus, one has to solve (27) with k_j replaced by ik_j. The ground-state energy is then defined by ($L < 0$: positive effective mass)

$$E_b = 2|L|(2 - \cos \chi_1 - \coth k_b) \tag{28}$$

where k_b satisfies (27) under the replacement indicated. There also exists an excited bound state, the energy of which is symmetric to that of the ground state with respect to the continuous spectrum of the discrete system. For the continuous model of the right-angle

bend waveguide, where the electron-energy spectrum is unrestricted, there is only one bound state below the bottom of the continuous spectrum.

Calculations of the bound-state energy spacing from the propagation threshold energy $E_{th} = 2|L|(1 - \cos\chi_1)$ are presented in table 1 (together with the result for the continuum limit) in units of E_{th} and $2|L|$. As can be seen, the difference in the ground-state energy between the discrete and continuum models is already quite small for comparatively narrow waveguides, $N = 10$–20. Note also that, in the one-mode approximation, $(E^c_{th} - E^c_b)/E^c_{th} = 0.054$ ($E^c_{th} = \hbar^2 k^2_{th}/2m^*$, $k_{th} = \pi/w$, $w = a(N + 1)$ is the wire width, the superscript c labels the continuum model, CL). In the two-, three- and four-mode approximations, this quantity equals to 0.063, 0.065, 0.067, respectively. This exemplifies the convergence of the computational procedure used. For the 'wavevector' of the bound state, $K_b/k_{th} = \sqrt{E_b/E_{th}}$, we obtain 0.9646, which is a more accurate value than 0.96 [1].

Table 1. Bound-state energies in the right-angle bend.

N	$[(E_{th} - E_b)/E_{th}] \times 10$	$[(E_{th} - E_b)/\|2L\|] \times 10$
2	0.186	0.102
3	0.344	0.106
4	0.439	0.087
5	0.500	0.069
10	0.622	0.025
15	0.658	0.013
20	0.674	0.0075
CL ($N = \infty$)	0.696	0
CL [1]	0.784	0

5. Computational results and discussion

We now turn to characterizing the scattering properties of a right-angle bend in the continuum model. The use of (18)–(21) considerably simplifies computations of the scattering probabilities R_{jj_0} and T_{jj_0} with a large number of modes involved.

To get some idea about the microscopic picture of electron motion, one needs the mode transmission (reflection) coefficients (or scattering probabilities) which determine the efficiency of the mode transformation in the scattering region of electrons. The total transmission coefficient, $T_{j_0} = \sum_j T_{jj_0}$ for the fundamental-mode propagation, $j_0 = 1$, was calculated by Weisshaar and co-workers [7]. Those calculations are shown by the dotted curve in figure 2(a) (all characteristics are given here as functions of q_1, the longitudinal wavevector in the first subband, which is scaled with the propagation threshold wavevector k_{th}, $q_1 = k_1 a^{-1}/k_{th}$). Full curves in figures 2(a)–(c) represent contributions to the total j_0th mode transmission probability, coming from all other modes which can propagate in the waveguide at the given energy. We see that the first-mode wave in the input lead effectively converts into the second- (third-) mode wave in the output lead in the energy region of the second (third) subband. The right-angle waveguide also possesses a high-mode transformation capacity of the second-mode wave into the third-mode wave and vice versa in the second and third subbands, see identical ($T_{23} = T_{32}$) curves in figures 2(b) and (c).

Since the injection of individual modes is hardly accessible in a transport experiment, the measurable quantities are the total average transmission coefficient $T^{av} = N_0^{-1} \sum_{j_0=1}^{N_0} T_{j_0}$ (which determines the conductivity of degenerated electrons in a two-terminal structure [12, 13]) and the distribution of outgoing electrons among all N_0 modes available

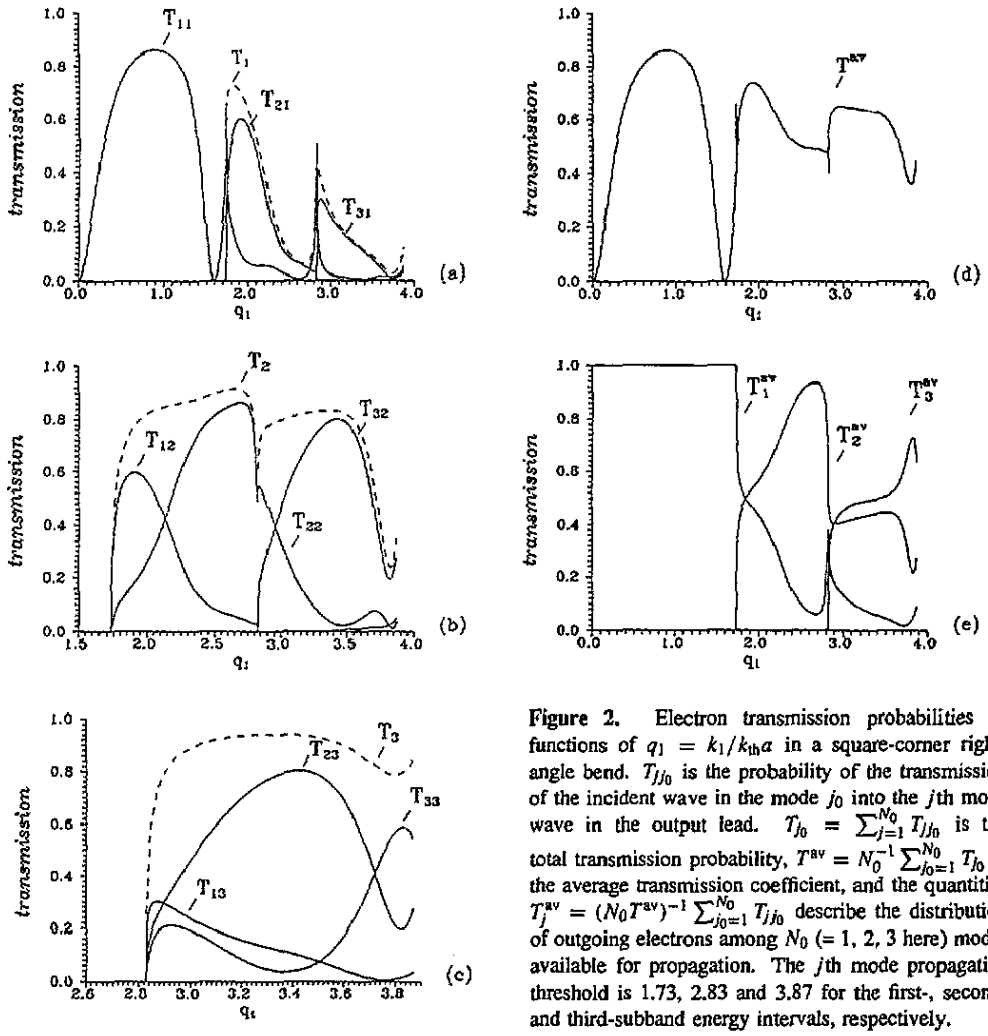

Figure 2. Electron transmission probabilities as functions of $q_1 = k_1/k_{th}a$ in a square-corner right-angle bend. $T_{j j_0}$ is the probability of the transmission of the incident wave in the mode j_0 into the jth mode wave in the output lead. $T_{j_0} = \sum_{j=1}^{N_0} T_{j j_0}$ is the total transmission probability, $T^{av} = N_0^{-1} \sum_{j_0=1}^{N_0} T_{j_0}$ is the average transmission coefficient, and the quantities $T_j^{av} = (N_0 T^{av})^{-1} \sum_{j_0=1}^{N_0} T_{j j_0}$ describe the distribution of outgoing electrons among N_0 (= 1, 2, 3 here) modes available for propagation. The jth mode propagation threshold is 1.73, 2.83 and 3.87 for the first-, second- and third-subband energy intervals, respectively.

for propagation, $T_j^{av} = N_0^{-1} \sum_{j_0=1}^{N_0} T_{j j_0}/T^{av}$. The latter quantity characterizes the system as a filter of electrons.

Figure 2(*d*) shows that two regions of a high conductance of the right-angle bend are separated by a well pronounced valley of a low (zero at the point $q_1 = 1.6$) conductance—a promising property for device applications. In any case, as distinct from the circular right-angle bend [6], the square-corner right-angle bend should be regarded in a quantum device technology as a device itself rather than a passive interconnection of different parts of a nanocircuit.

As seen from figure 2(*e*), the fundamental-mode population is considerably suppressed in the transmitted flux when the electron energy increases. At the same time, the second and third modes are nearly equally populated except the region close to the fourth-mode opening. Thus, the electron filtering can be efficient within the second-subband energy interval.

Let us consider briefly the dependence of the through-right-angle-bend transmission on the shape of the discontinuity region 'in'. As was mentioned above, the two-terminal structures are expected to possess the resonant reflection of the first-mode wave, which,

in the case of the discussed structure, is realized at $q_1 = 1.6$, i.e. the energy of the resonant reflection of electrons $E_{res} \approx 3.6 \times E_{th}^{c}$. The effect is a sequence of the interference of electron waves in the discontinuity region and, therefore, depends on its shape. Modifications of this shape can lead to considerable changes of the resonant reflection energy as well as of the form of the waveguide transmission spectrum. Some examples of this dependence are presented in figure 3, where the fundamental-mode transmission spectrum of modified right-angle bends (figures 3(*b*)–(*d*) are compared with its original form (figure 3(*a*)). An extension of the area 'in' by an additional stub may result (depending on the stub length) in a shift, broadening and enlarging the number of resonances. Analogous changes of the transmission spectrum can be caused by supplementing the structure with two additional stubs, which extend both input and output leads.

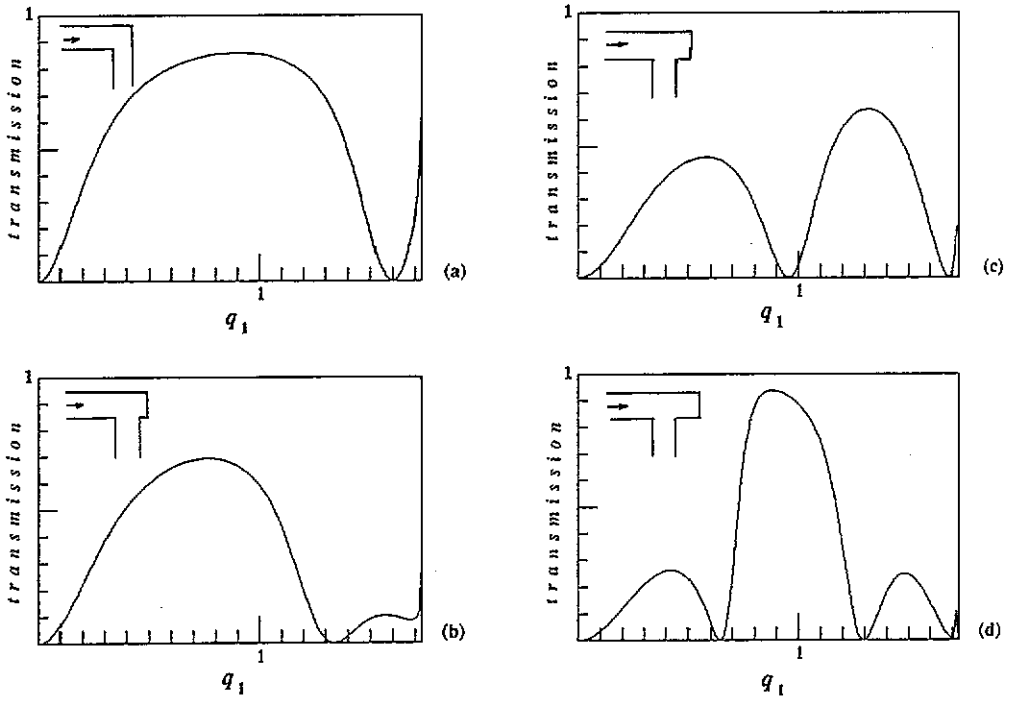

Figure 3. The transmission probability in a square-corner right-angle bend (*a*) and its modifications (*b*)–(*d*). The length of the additional stub shown in the inserts of (*b*), (*c*) and (*d*) is $0.2w$, $0.5w$ and w, respectively.

It is also of importance for our understanding of a possible role of waveguides connecting different parts of a circuit, to compare the present results with those for a circular right-angle bend [6]. If we change the bend shape in the way shown by dotted curve in figure 1, we obtain the structure with zero inner radius of the bend curvature and with the outer radius equal to the waveguide width. There are several noticeable distinctions in properties of such a circular right-angle bend. The most striking of them is the monotonic increase of the transmission within the first subband which leads to a nearly perfect fundamental-mode transmission through the circular right angle except for energies very close to the propagation threshold in the channel [6]. Thus, the precise geometry of the bend is crucial for determining its transport properties.

As has been just demonstrated, the transport (or device) characteristics of a right-angle waveguide are prospective and appealing to be realized. But we see a serious warning about difficulties in this method in the drastic dependence on the bend shaping which has been pointed out above. It is likely that properties of other square-corner discontinuities are not less sensitive to the corner smoothing.

6. Conclusion

An explicit form of equations, which gives a complete description of the ballistic electron transport in a square-corner right-angle waveguide, has been derived. On this basis, general transport properties of the system have been proved. To our knowledge, this has never been done analytically. The S-matrix equations (presented in the canonical form which is general for square-corner discontinuities) have been reduced to the triangular form with the coefficients defined by simple recurrent relations. In fact, this gives the explicit (exact) solution of the scattering problem for the discrete model of the waveguide with (arbitrary) N-site width and the solution for the standard continuum model of the waveguide in the N-mode approximation. The solution obtained simplifies considerably computations for the square-corner right-angle bend and relevant structures. Quantities of physical interest, the ground-state energy and the reflection and transmission probabilities up to the fourth-mode opening, have been calculated in the framework of the original method. A non-trivial dependence of the degenerate electron-gas conductance on the Fermi energy and the electron filtering in right-angle waveguides are predicted.

References

[1] Schult R L, Ravenhall D G and Wyld H W 1989 *Phys. Rev.* B **39** 5476
[2] Sols F, Macucci M, Ravaioli U and Hess K 1989 *J. Appl. Phys.* **66** 3892
[3] Kirzcenow G 1989 *Phys. Rev.* B **39** 10452
[4] Baranger H U 1990 *Phys. Rev.* B **42** 11478
[5] Lent C S and Kirkner D J 1990 *J. Appl. Phys.* **67** 6353
[6] Lent C S 1990 *Appl. Phys. Lett.* **56** 2554; **57** 1678
[7] Weisshaar A, Lary J, Goodnick S M and Tripathi V K 1989 *Appl. Phys. Lett.* **55** 2114
[8] Berggren K-F and Ji Zhen-li 1990 *Superlatt. Microstruct.* **8** 59; 1991 *Phys. Rev.* B **43** 4760
[9] Gaididei Yu B, Malysheva L I and Onipko A I 1992 *Phys. Stat. Sol. (b)* **172** 667
[10] Gaididei Yu B, Malysheva L I and Onipko A I 1992 *J. Phys.: Condens. Matter* **4** 7103
[11] Wu H, Sprung D W L and Martorell J 1992 *Phys. Rev.* B **45** 11960
[12] Landauer R 1957 *IBM J. Res. Develop.* **1** 223
[13] Büttiker M 1988 *IBM J. Res. Develop.* **32** 317